Sizing and Energy Management of a Hybrid Locomotive Based on Flywheel and Accumulators

Amine Jaafar, Cossi Rockys Akli, Bruno Sareni, Xavier Roboam, Alain Jeunesse

Sizing and Energy Management of a Hybrid Locomotive Based on Flywheel and Accumulators

Amine Jaafar, Cossi Rockys Akli, Bruno Sareni, Xavier Roboam, and Alain Jeunesse

***Abstract*—The French National Railways Company (SNCF) is interested in the design of a hybrid locomotive based on various storage devices (accumulator, flywheel, and ultracapacitor) and fed by a diesel generator. This paper particularly deals with the integration of a flywheel device as a storage element with a reduced-power diesel generator and accumulators on the hybrid locomotive. First, a power flow model of energy-storage elements (flywheel and accumulator) is developed to achieve the design of the whole traction system. Then, two energy-management strategies based on a frequency approach are proposed. The first strategy led us to a bad exploitation of the flywheel, whereas the second strategy provides an optimal sizing of the storage device. Finally, a comparative study of the proposed structure with a flywheel and the existing structure of the locomotive (diesel generator, accumulators, and ultracapacitors) is presented.**

***Index Terms*—Battery, energy-management strategy, energy storage, flywheel, hybrid locomotive.**

NOMENCLATURE

P_{DG}	Diesel generator power.
P_{DGref}, $P_{\mathrm{DG\,max}}$, P_{DGnom}	Reference, maximal, and nominal diesel generator power.
E_{DG}	Diesel generator energy.
SFC	Specific fuel consumption.
Q_{fuel}	Consumed fuel quantity by the diesel generator.
Q_{CO2}	Dioxide carbon quantity emitted by the diesel generator.
η_{DG}	Diesel generator converter efficiency.
P_S	Instantaneous power exchanged by the storage elements (index "s" corresponds to "BT" for the battery, "SC" for ultracapacitors, and "FW" for the flywheel).
P_s^r	Instantaneous real power exchanged by the storage elements.
P_{Sref}	Reference power for storage elements.
$P_{S\,dch\,\max}/P_{S\,ch\,\max}$	Maximal charge/discharge power for the storage elements.
E_S, $E_{S\,\max}$	Instantaneous and maximal stored energy of the storage elements.
SOC_S	Storage element state of charge.
η_S	Storage element energy efficiency.
P_{LOC}	Locomotive power mission.
$P_{\mathrm{Loc-LF}}$	Total mission low-frequency part and flywheel filtered losses.
p_{FW}	Flywheel losses.
$p_{\mathrm{FW-LF}}$	Low-frequency part of flywheel losses.
ΔP_{FW}	Charge power excess for the flywheel.
F_g	Cutoff frequency.
P_{FWref0}	Power reference for the flywheel before P_{FWS} injection.
P_{FWS}	Flywheel secondary mission.
R_{FW}	Flywheel power reserve.
P_{BTref0}	Battery mission before the injection of P_{FWS}.
Ω_{DG}, Ω_S, Ω_Σ	Diesel generator, storage element, and global system volume.
$\mathrm{NP_{BT}}$, $\mathrm{NS_{BT}}$	Number of parallel and series battery cells.
NP_S, $\mathrm{NS_{SC}}$	Number of parallel and series ultracapacitor cells.
DOD	Storage element depth of discharge.
c_F	Number of cycles to failure.
N_{CYCLE}	Total number of cycles.
w_{CYCLE}	"cycle weight."
$\mathrm{LFT_{BT}}$	Global battery stress estimator.
S_{ex}	Existing solution for the hybrid locomotive.
S_{FW1}, S_{FW2}	Flywheel-based solution with basic and optimized management strategies.

A. Jaafar, B. Sareni, and X. Roboam are with the Institut National Polytechnique de Toulouse, Université de Toulouse, 31071 Toulouse, France (e-mail: jaafar@laplace.univ-tlse.fr; bruno.sareni@laplace.univ-tlse.fr; roboam@laplace.univ-tlse.fr).

C. R. Akli is with ALSTOM Transport Tarbes, 65600 Semeac, France (e-mail: akli@laplace.univ-tlse.fr).

A. Jeunesse is with the French National Railways Company, Centre d'Ingénierie du Matériel, 72100 Le Mans, France (e-mail: alain.jeunesse@sncf.fr).

I. INTRODUCTION

BY COMPARISON with aircraft and automotive systems, railway transport is recognized as being a sustainable mode of transport with reduced carbon emissions.

Indeed, most passenger trains, particularly in France, where 85% of all passenger trains are high-speed trains (i.e., TGV), are electrically fed [1]. However, for particular segments such as sorting and local sideboards, driving missions are generally achieved by diesel locomotives. In such cases, the diesel engine operates more than 60% of the time at slow motion [2]–[4]. This leads to an excess in fuel consumption, polluting broadcasts, and noise [5]–[8]. Diesel-electric hybridization then establishes an interesting solution before being completely "zero fuel" by means of new technologies of generators (fuel cells, etc.). It allows answering simultaneously economical and environmental objectives by reducing, on the one hand, the fuel burn and, on the other hand, CO_2 emissions. Energy-storage elements mostly used to hybridize diesel locomotives are accumulators, flywheels, and ultracapacitors. "NewEnergy train (NE@Train)" [9] is the first railway hybrid locomotive put on rails. This suburb train has been built by the Japanese company JR-EAST. It is composed of a 230 kW diesel generator associated with 10 kW lithium-ion batteries [10]. It allows a 20% reduction in the fuel burn and a 50% reduction in polluting broadcasts, compared with a full-diesel locomotive.

The Canadian company RailPower (RP) is the first railway builder producing hybrid locomotives assembling diesel and accumulator batteries in an industrial way [2], [3]. It commercializes two groups of locomotives. The Green Goat group of sorting is based on a 200 kW diesel generator (against 1500 kW for an equivalent diesel locomotive) and a great pack of batteries (Pb-1200 Ah under 600 V DC). The group RP of operation in two versions (RP20BH and RP20BD) embeds two or three 500 kW diesel generators and batteries of the same technology.

The CITADIS of Rotterdam is a hybrid streetcar Catenaries-Flywheel fabricated by the railway designer Alstom. It is dedicated to crossing the Erasmus bridge of Rotterdam without catenaries. Alstom also built, in Nice, France, a hybrid CITADIS with NiMH batteries for the crossing of Garibaldi and Massena places without catenaries [11].

In this context, the Energy Efficient and Environmentally Friendly Train Platform (PLATHEE Project) has been created between the French National Railways Company (SNCF), the Laboratory on Plasma and Conversion of Energy (LAPLACE), and several other French partners, such as ALSTOM, INRETS, SOCOFER, SOPRANO, 2HENERGY, and ERECTEEL [12]. This project is focused on the design, i.e., architecture, sizing, and energy management of an autonomous hybrid locomotive. Existing equipment used by the SNCF was based on a BB63000 diesel locomotive dedicated to carry out missions of sorting and local sideboards and to help in the absence of catenaries. This locomotive is powered by four electric motors fed by a 610 kW diesel generator. A former study consisted of replacing the diesel engine with a smaller diesel engine with batteries of accumulators and ultracapacitors as energy-storage elements [1]. Complementarily to the previous design, the current study proposed in this paper has the objective to investigate the possibility of implanting a flywheel device on the future hybrid locomotive.

This paper is organized as follows: First, power-flow-based modeling is presented for the energy-storage elements. Second, the principle of the energy-management strategy based on a frequency approach is explained. The integration of a flywheel on the hybrid locomotive in association with the diesel generator and the accumulator batteries is then studied by considering two different energy-management strategies. Finally, a comparative study is carried out between the proposed solution with a flywheel and that existing with ultracapacitors.

II. Existing Solution of the Hybrid Locomotive

The existing architecture of the hybrid locomotive is shown in Fig. 1. It has been built from an existing BB63000 diesel locomotive devoted to carrying out sorting or local sideboard missions and help in the absence of catenaries. This locomotive is moved by four dc electric motors fed by a diesel generator of 610 kW rated power. One first issue was to replace the diesel generator with a smaller diesel generator by building a hybrid system by inserting the batteries of accumulators and ultracapacitors as energy-storage elements. A first study [1], [4] then allowed the sizing of the locomotive with a diesel generator of 215 kW rated power, 200 kWh of batteries (1200 nickel cadmium cells of 135 Ah/1.2 V), and 7 kWh of ultracapacitors (1600 cells of 5000 F/2.5 V). An energy-management strategy has been proposed based on a frequency approach. The batteries are distributed in four parallel blocks of 300 cells in series; ultracapacitors are shared in eight parallel blocks of 200 cells in series. These blocks are connected to a 540 V DC bus through power converters.

III. Flywheel Energy Storage

Flywheel energy storage has been used since antiquity. In the past few decades, it has equipped electromechanical applications to smooth the electric power demand or secondary power supply to secure cases of electric cuts of weak duration. It is also used in uninterruptible power supplies where the short-duration power changes damage the lifetime of the batteries. In the context of autonomous energy production, flywheels are used in the field of transport and in spatial applications for energy transfer and, particularly, to stabilize or drive satellites (gyroscopic effect) [13]. Flywheel energy storage is characterized by its important lifetime (typically 20 years) [14], [15]. However, its main drawback is security issues, in particular for embedded systems.

The main flywheel energy storage devices are shown in Fig. 2. The flywheel is usually a cylindrical mass that allows kinetic energy to accumulate. It turns with high rotation speeds with reduced losses due to magnetic bearings. The motor/generator, coupled with a static converter, is used for the electromechanical energy conversion system. These elements are placed in a safety and vacuum envelope. This last one is waterproof and under a vacuum of air to minimize friction losses [16], [17].

IV. Power Flow Modeling

The power flow model is a macroscopic modeling particularly dedicated to a system approach for energetic devices. It treats energy and power exchanged by the storage elements and

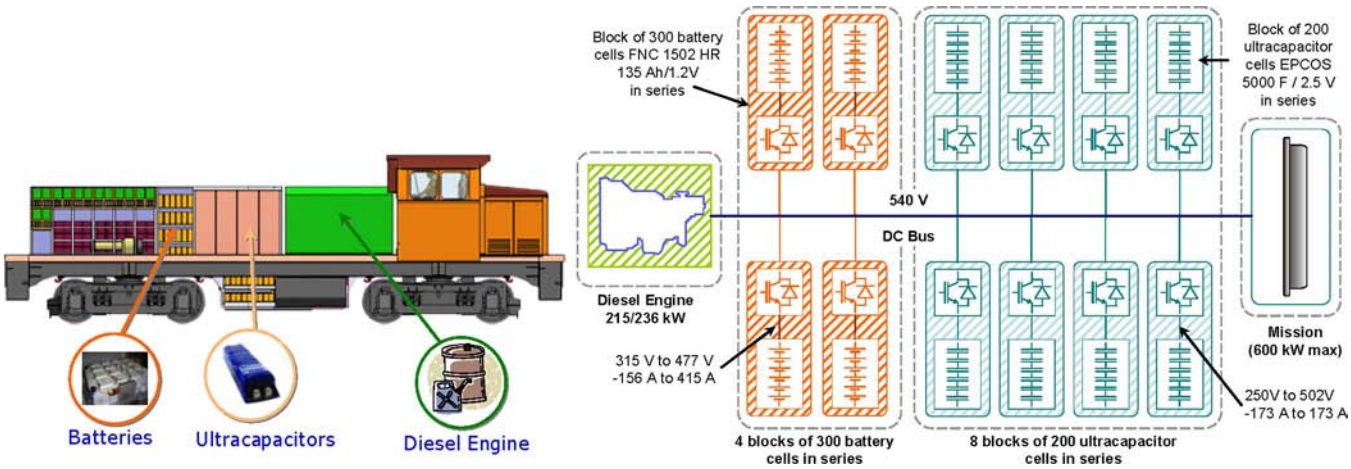

Fig. 1. Initial architecture of the hybrid locomotive.

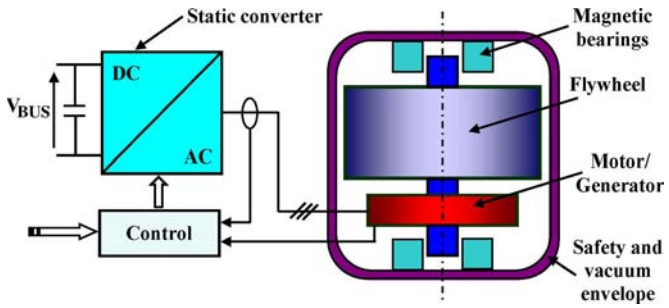

Fig. 2. Initial architecture of the hybrid locomotive.

the whole system. It also represents a sizing model. In fact, it allows determination of the energy size of storage elements without taking into account their electrical characteristics or their interconnection architecture (i.e., series/parallel assembling). This model offers the advantage of minimizing computational cost particularly as long-term driving missions are treated in this railway transport application: 5 s of computation time are needed to simulate 6 h of driving mission, compared with 60 h to simulate a complete "instantaneous electric model" [1].

A. Power Flow Model of the Diesel Generator

The power flow model of the diesel generator is shown in Fig. 3. From the diesel generator power reference P_{DGref}, it allows us to obtain the "actual" diesel generator power P_{DG}, the corresponding energy E_{DG}, the quantity of fuel consumed Q_{fuel}, and the corresponding quantity of emitted carbon dioxide Q_{CO2}. The parameters of this model are the converter efficiency associated with the diesel generator (typically $\eta_{\mathrm{DG}} = 96\%$), the diesel power limit $P_{\mathrm{DG\,max}}$, and the specific fuel consumption (SFC) characteristic. This characteristic has been extrapolated with a five-order polynomial approximation as a function of the diesel generator power as follows [1]:

$$\mathrm{SFC}(P_{\mathrm{DG}}) = \mathrm{SFC}_N \sum_{i=0}^{5} b_i \left(\frac{P_{\mathrm{DG}}}{P_{\mathrm{DGN}}}\right)^i \qquad (1)$$

where the polynomial coefficients are $b_0 = 1.94$, $b_1 = -6.44$, $b_2 = 18.57$, $b_3 = -27.22$, $b_4 = 19.72$, and $b_5 = 1.94$. P_{DGN} denotes the rated power of the diesel generator, and SFC_N represents the SFC at this power estimated at 202.45 g/kW. The previous relationship has been validated for three diesel engines of the Fiat Powertrain Technologies Group [18], i.e., 125 kW N67 TM2A, 236 kW C78 TE2ES, and 335 kW C13 TE2S. It should be noted that the SFC is minimum when the diesel engine operates at its nominal power P_{DGN}. Therefore, the energy-management controller tends to maintain the diesel generator power reference close to this power or to stop it. Note also that the maximal diesel engine power is considered to be 10% higher than the nominal power.

The emitted quantity of CO_2 in kilograms (Q_{CO2}) is directly proportional to the consumed fuel quantity in liters (Q_{fuel}) and is estimated as follows [19]:

$$Q_{\mathrm{CO2}} = 2.66 Q_{\mathrm{fuel}}. \qquad (2)$$

B. Power Flow Model of the Storage Elements

Fig. 4 describes the power flow model of the storage elements. The model is identical for batteries, ultracapacitors, and flywheel; therefore, the s index in Fig. 4 can be replaced by BT for the battery pack, SC for the ultracapacitor pack, and FW for the flywheel.

P_{Sref} is the power reference of the storage element computed from the energy-management strategy controller. This power has some limitations, depending, on the one hand, on the maximal power of charge $P_{S\,ch\,\max}$ and the acceptable storage element discharge $P_{S\,dch\,\max}$ and, on the other hand, on its state of charge ($\mathrm{SOC}_{\min}$ and $\mathrm{SOC}_{\max}$). Various losses are considered by introducing the energy efficiency (η_S if $P_S < 0$ and $1/\eta_S$ if $P_S > 0$). Note that positive power values are equivalent to discharging the storage device, whereas negative power values correspond to charging a storage device.

The storage element state of charge SOC_S is defined as the ratio between the instantaneous stored energy E_S and the maximal energy that can be stored $E_{S\,\max}$ ($\mathrm{SOC}_S(\%) = 100 \times E_S / E_{S\,\max}$). The energy calculation of the storage elements E_S is

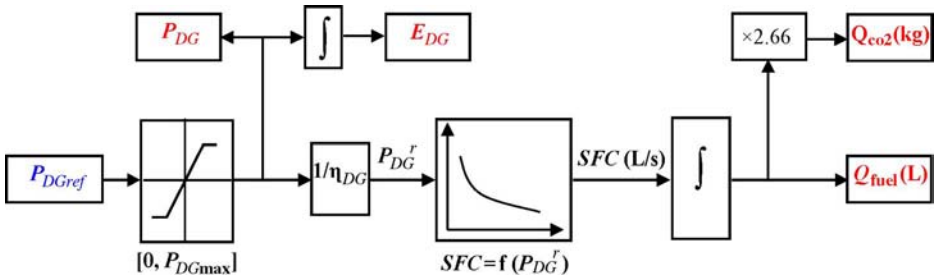

Fig. 3. Power flow model of the diesel generator.

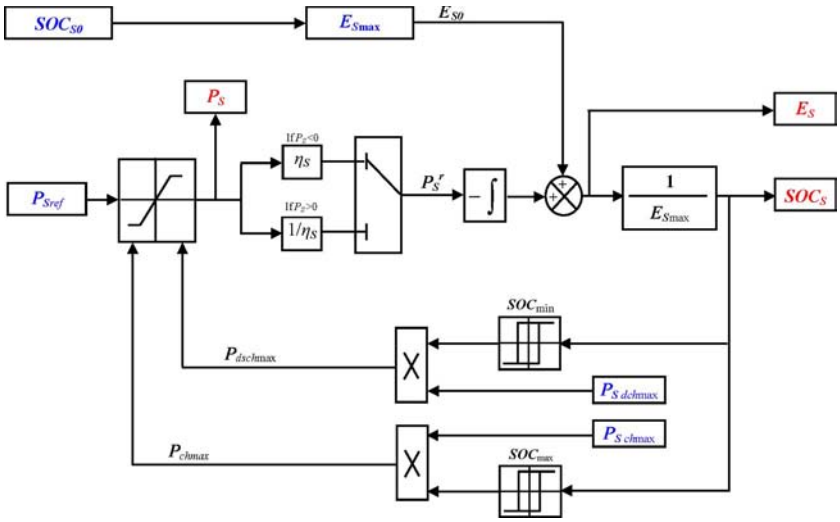

Fig. 4. Power flow model of a storage element pack (flywheel, batteries, or ultracapacitors).

TABLE I
PARAMETERS OF THE BATTERY, ULTRACAPACITOR, AND FLYWHEEL POWER FLOW MODELS

	Ultracapacitors	Batteries	Flywheel
Efficiency (including the converter efficiency)	η_{SC}=91%	η_{BT}=80%	η_{FW}=90%
Discharge limit $P_{sdchmax}$	475 kW	380 kW	325 kW
Charge limit P_{schmax}	–475 kW	–97.2 kW	–325 kW

carried out from its instantaneous real power P_s^r and its initial state of charge SOC_{S0} according to the following relation:

$$E_S(t) = E_{S0} - \int_0^t P_S^r(\tau)d\tau. \quad (3)$$

This energy then allows the calculation of the state of charge of the storage element SOC_S.

The parameters of this model and their values are given in Table I. Note that the total energetic capacity of a pack depends on the total number of cells and on the capacity of each cell.

The main characteristics of the flywheel device considered in the study case of the hybrid locomotive are given as follows: a maximal charge/discharge power (±325 kW), a maximal storage energy capacity $E_{\mathrm{FW\,max}} = 5.33$ kWh (4 kWh as useful energy), and the speed varying between 11 000 and 22 000 r/min.

Technological data values corresponding to EPCOS 5000 F/2.5 V ultracapacitor cells and Hoppecke FNC 1502HR battery cells of 135 Ah, which are used in the PLATHEE Project, are detailed in [20].

V. ENERGY-MANAGEMENT STRATEGY BASED ON A FREQUENCY APPROACH

To determine the mission part of each storage element, an energy-management strategy based on a frequency approach was presented in [4] in the case of hybridization with batteries and ultracapacitors. It is similarly used here with flywheel storage. Its principle resides in the following rule:

The fast storage elements SC (ultracapacitors) or FW (flywheels) assure high-frequency components of the mission (see Fig. 5). The energy source diesel generator DG operates as often as possible at its nominal power, and the remainder of the mission is devoted to the batteries BT. In fact, for the actual system operation, a more complex "stop-and-go" strategy is adapted for diesel generator management. Indeed, this latter source has to be switched off when the demanded power is low regarding storage element SOC_S.

The "stop-and-go" allows determination of the diesel generator control reference based on the low-frequency part of the mission $(\mathrm{PDG} + \mathrm{PBT})$ and on the battery state of charge $\mathrm{SOC}_{\mathrm{BT}}$ as follows:

If $(P_{\mathrm{DG}} + P_{\mathrm{BT}}) > P_{\mathrm{BT\,dch\,max}}$ or $\mathrm{SOC}_{\mathrm{BT}} < 90\%$, then "Start DG" = 1; otherwise, "Start DG" = 0.

A hysteresis control process is introduced to fulfill a minimal operating duration before stopping and a minimal idling duration before starting.

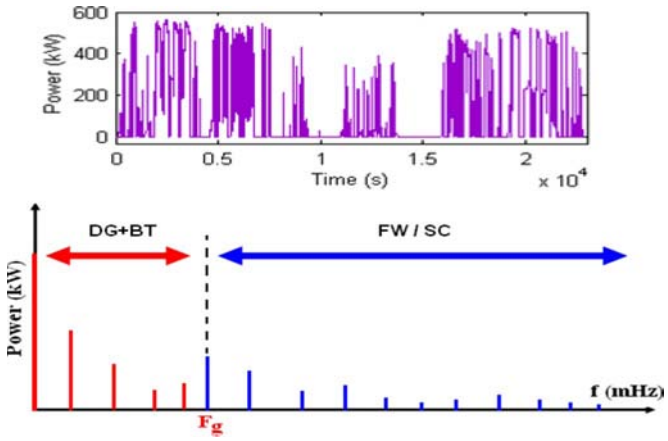

Fig. 5. Mission distribution according to a frequency axis.

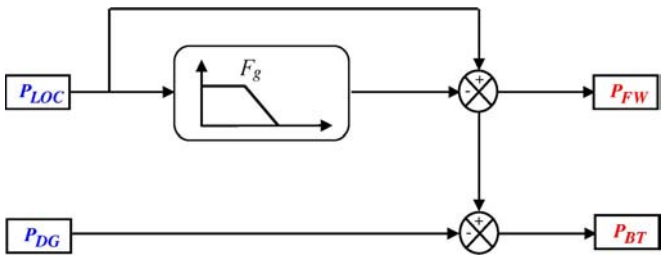

Fig. 6. Basic principle of the frequency-based energy-management strategy.

From the whole locomotive power mission P_{LOC}, a high-pass filter allows sharing the high-frequency part, which is devoted to the flywheel (case of architecture DG, BT, and FW). The mission of the batteries P_{BT} is obtained by subtracting the diesel generator power from the lower frequency part of the locomotive power mission (see Fig. 6).

This management strategy secures the compatibility between the frequency components of the mission and the intrinsic characteristics of the different sources.

1) The nominal power is the optimal operating point of the diesel generator. At this point, the fuel burn is minimum, and the atmospheric pollution CO_2 is also minimized [21].
2) Batteries are actual energy sources providing few slow dynamic cycles (about 1000 cycles). Furthermore, batteries are subject to aging, and the best way to prolong their lifetime is to prevent them from fast dynamic currents and a high number of cycles.
3) Contrarily to batteries, ultracapacitors are able to absorb fast dynamic currents and to provide a significant number of cycles (typically 500 000 cycles) [22].
4) Flywheels are placed between these last two elements and characterized by a "quasi-infinite" number of fast dynamic cycles of charge and discharge [23].

Table II gives a summary of the characteristics of the different sources:

The cost of the different energy sources is not mentioned in the table as it depends on many parameters, such as the costs related to maintenance, lifetime, and purchasing. More details can be found in [24].

TABLE II
CHARACTERISTICS OF THE DIFFERENT ENERGY SOURCES

	Diesel Generator	Batteries	Ultracapacitors	Flywheel
Specific energy (Wh/kg)	93	20-200	1-10	10-95
Specific power (W/kg)	94	5-20	1000-3000	2000-4000
Charge time	-	1-5h	1-30s	>15s
Discharge time	-	0.3-3h	1-30s	>few min
Number of cycles	-	2000	$>10^5$	$>10^5$

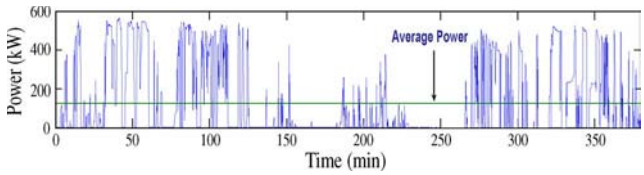

Fig. 7. Typical difficult locomotive mission profile.

VI. HYBRID LOCOMOTIVE WITH DIESEL GENERATOR, BATTERIES, AND FLYWHEEL

In this section, we study the hybridization of the locomotive, which consists of removing the existing ultracapacitors and only considering the diesel generator (215/236 kW) with the batteries and the flywheel. Our objective is to define a management strategy guaranteeing optimal sizing and operation of the locomotive. In the following, we propose two energy-management strategies confirmed by a power flow model. Our study is carried out for the mission of Fig. 7 that is considered as one of the most critical in terms of power/energy constraints: This latter mission is taken as reference in the design process.

A. Basic Management Strategy: The Flywheel Only Supplies High-Frequency Harmonics

1) Principle: This first "basic" management strategy is identical to that one applied to the hybrid locomotive with ultracapacitors. The flywheel supplies the high-frequency part of the mission, and the rest is shared toward the diesel generator and the batteries. As long as the "low-frequency" power part is lower than the nominal power of the diesel generator, the later satisfies the required mission and also charges the batteries. In the opposite case, the diesel engine operates at its nominal power, and the batteries guarantee the rest of the mission. Consequently, it is supposed, at first, that the diesel engine always supplies its nominal power P_{DGnom}. This power will be deduced from $P_{\mathrm{Loc-LF}}$ (the low-frequency part of the total mission and the filtered losses of the FW) to determine the reference mission of the batteries P_{BTref}. A compensation loop of the low-frequency part of the flywheel losses is added.

Cutoff frequency F_g is chosen so that the flywheel does not reach saturations in discharge while staying in the frequency domain of the batteries. However, saturations in charge are allowed. In this case, the charge power excess ($\Delta P_{\mathrm{FW}} = P_{\mathrm{FWref}} - P_{\mathrm{FW}}$) is sent to the diesel generator to relieve it. Such

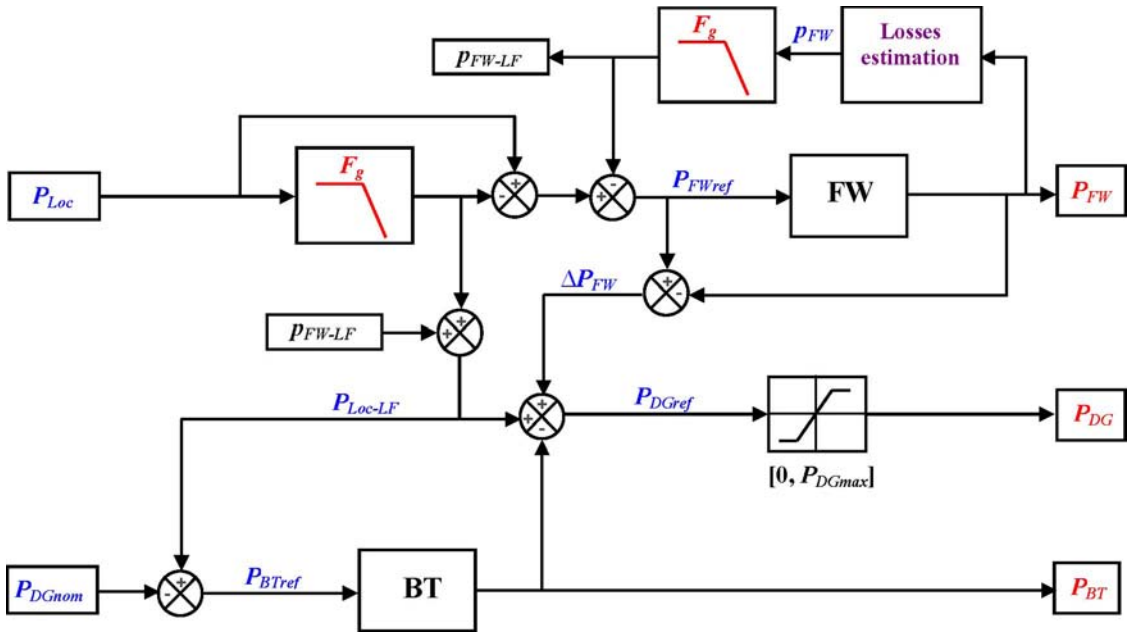

Fig. 8. Synoptic plan of the basic management strategy.

a power flow model of the energy-management strategy based on a frequency approach is shown in Fig. 8.

By sweeping the frequency axis, we notice that only the cutoff frequency is responsible for the flywheel power use. To avoid the power saturations in discharge, the minimal cutoff frequency must be increased at $F_g = 27$ mHz, instead of the 5 mHz initially used with ultracapacitors. To comply with the reference mission, the number of batteries cells is then initially increased to 1312, instead of 1200. Remember that the useful energy stored in the considered flywheel is only 4 kWh, whereas that for utracapacitors is 7 kWh.

2) Simulation Results: The simulation results show that the flywheel fulfills its reference mission, except for some acceptable saturations of charge [see Fig. 9(a)]. The state of charge shown in this figure proves that the flywheel saturation is only due to power demands while no energy saturations are observed. This storage device is then able, with this frequency of 27 mHz, to comply with all the required energy states during this reference mission. The energy versus power cycles of the flywheel in the Ragone's plan and its operating limit area are also given in Fig. 9(a). This figure illustrates the behavior of the flywheel and the temporal evolution of the corresponding trajectories in Ragone's plan through a color code. Indeed, the scale of time is represented by various colors going from the dark blue at the beginning of the mission to the red at the end of the simulation. Initially, the flywheel is totally charged ($\mathrm{SOC_{FW}} = 100\%$), and its energy is then equal to 5.33 kWh. By going through the complete mission, its state of charge does not go below 77.2%, which corresponds to a stored energy of 4.1 kWh. This value is obviously superior to its minimal limit of discharge (1.33 kWh). Thus, one can conclude that the flywheel is not well exploited in terms of stored energy through this "basic" energy strategy management.

3) Comparison—Architecture DG+BT+SC/DG+BT+FW: The previous study has shown that flywheels can replace ultracapacitors under the condition of increasing the number of battery cells (112 cells have been added). The adequate cutoff frequency (27 mHz) is also higher than that used in the case of ultracapacitors (5 mHz). This leads to an increase in the frequency of the batteries cycles and the appearance of more microcycles that are able to decrease the battery lifetime.

By applying the same energy-management strategy ("basic" strategy) used in the case of ultracapacitors and by means of a power flow model, we showed that the hybrid architecture with flywheel allows fulfilment of the requirements of the hybrid locomotive with batteries and ultracapacitors in terms of power mission. However, the flywheel is not well exploited in terms of stored energy. In the next section, we propose a new management strategy allowing better use of the flywheel storage and allowing us to reach optimal sizing and operation of the locomotive.

B. Second Management Strategy: Optimized Management Strategy Based on a Frequency Approach

1) Principle: With the aim of a better exploitation of the flywheel, we shall keep the same management principle based on a frequency approach by introducing the following modification: Aside from the high-frequency mission P_{FWref0} considered as "the priority," the flywheel makes, if possible, a "secondary mission" P_{FWS} extracted from the low-frequency mission of the batteries, which relieves them. Concerning the FW reference power, the priority is always given to the high-frequency mission.

The secondary mission dedicated to the flywheel is determined in two steps. We first begin by defining a reserve for the flywheel power R_{FW} without any consideration of its state of charge (see Fig. 10). The issue here is to define the instantaneous distance between the high-frequency reference of the flywheel P_{FWref0} and the power limits, i.e., the maximal power $P_{\mathrm{FW\,dch\,max}}$ (325 kW) in the case of discharge

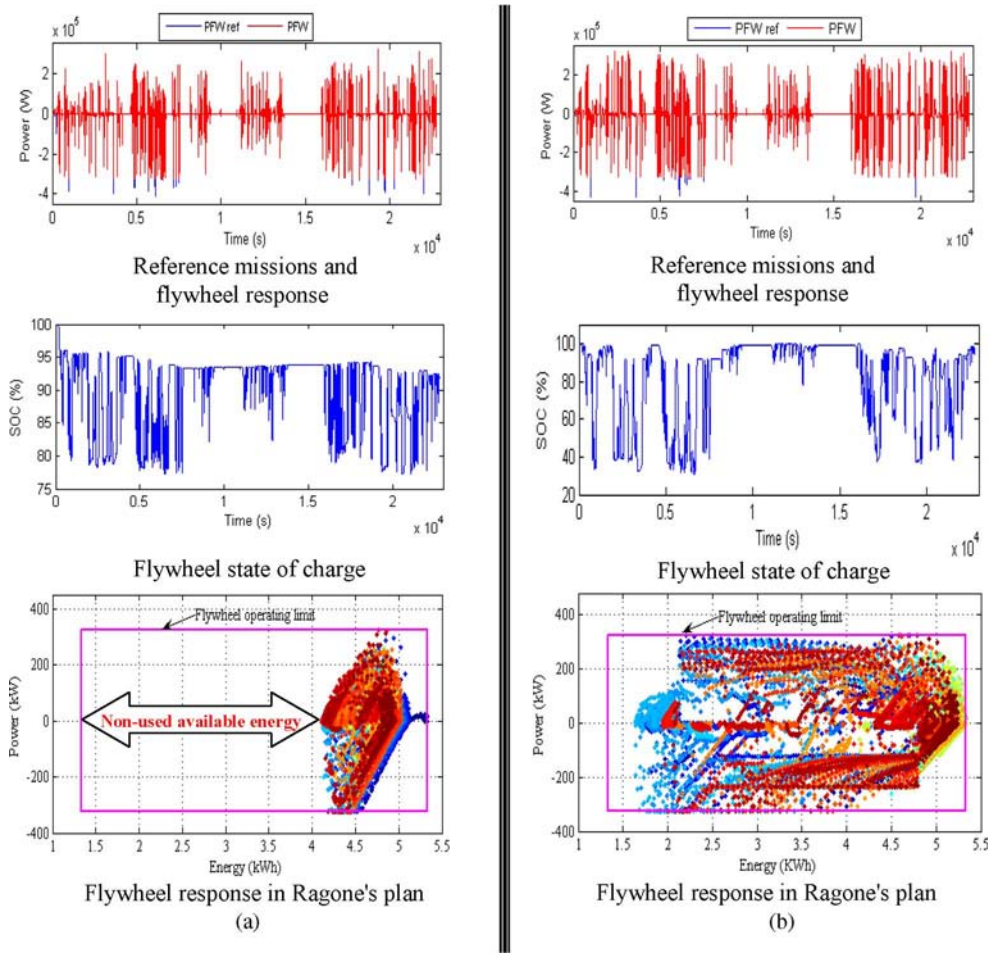

Fig. 9. (a) Basic and (b) optimized energy-management strategies.

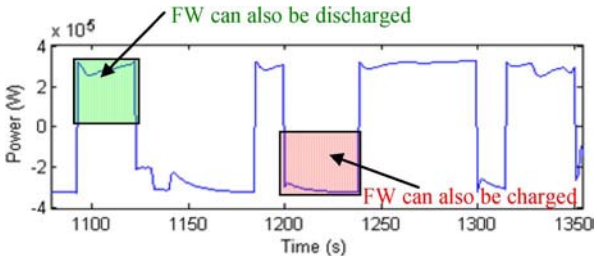

Fig. 10. Flywheel power reserve without any consideration of its state of charge.

and the minimal range $P_{\mathrm{FW\,ch\,max}}$ (-325 kW) in the case of charge.

Second, the battery reference mission P_{BTref0} (the mission of the battery before injection of P_{FWS}) is compared with the power reserve R_{FW} according to the principle given here.

- Case of a flywheel discharge: At this stage, control of the state of charge is necessary. A discharge of the flywheel to carry out the secondary mission can take place only if its state of charge is higher than 40%. This value constitutes a safety margin in terms of energy to guarantee the priority of the high-frequency mission P_{FWref0}.

  If power reserve R_{FW} is higher than P_{BTref0}, the battery is totally relieved (the reference of the battery after injection of P_{FWS} becomes $P_{\mathrm{BTref}} = 0$), and the flywheel secondary mission (P_{FWS}) is then equal to P_{BTref0} [see Fig. 11(a)]. In the opposite case, the flywheel supplies the whole reserve, and the batteries provide the necessary complement for mission fulfillment [see Fig. 11(b)].

1) Case of a flywheel charge: In this case, the flywheel is charged from the charge mission of the battery (the negative part of P_{FWref0}). This does not degrade the battery state of charge much, because the maximal energy that can be stored in the batteries (about 200 kWh) is significantly higher than that of the flywheel (4 kWh as useful energy). A charge of the flywheel, from the secondary mission, only takes place if its state of charge is lower than 90%; otherwise, priority is reserved for the high-frequency mission.

   If the power reserve RFW is lower than P_{FWref0} (i.e., greater in absolute value), we inhibit the battery charge $(P_{\mathrm{BTref}} = 0)$, and the secondary mission of the flywheel (P_{FWS}) is then equal to P_{FWref0} [see Fig. 12(a)]. In the opposite case [see Fig. 12(b)], P_{FWS} will be equal to R_{FW}, and the battery is less charged $(P_{\mathrm{BTref}} = P_{\mathrm{FWref0}} - R_{\mathrm{FW}})$.

   The synoptic scheme of this energy management based on a power flow model is shown in Fig. 13. It is similar to that used for the basic strategy, except for the block inserted to generate the secondary mission of the flywheel.

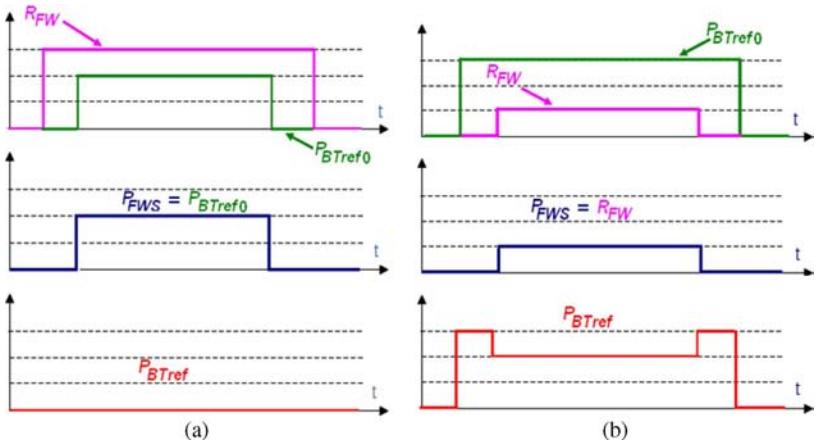

Fig. 11. Determination of the PFWS and the PBTref in the case of a discharge. (a) $R_{\mathrm{FW}} > P_{\mathrm{BTref0}}$. (b) $R_{\mathrm{FW}} < P_{\mathrm{BTref0}}$.

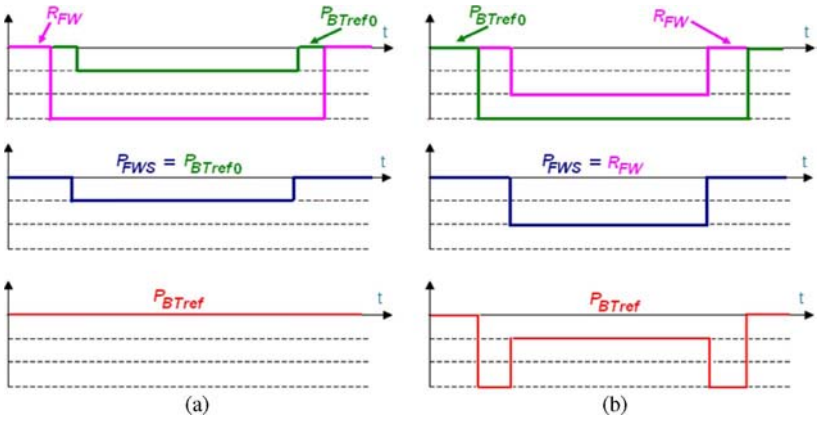

Fig. 12. Determination of the PFWS and the PBTref in the case of a charge. (a) $R_{\mathrm{FW}} < P_{\mathrm{BTref0}}$. (b) $R_{\mathrm{FW}} > P_{\mathrm{BTref0}}$.

2) Simulation Results: Simulations are made for the daily mission of the hybrid locomotive having a duration of 380 minutes and corresponding to the most critical mission in terms of power/energy demand. The cutoff frequency of the filter used inside the management process is chosen so that the flywheel does not admit saturations in discharge, whereas those in charge are acceptable. The minimal value to satisfy this condition is 17 mHz. Compared with the first basic management strategy ($F_g = 27$ mHz), the management filtering frequency is decreased. This decrease is in favor of the batteries, because the cycling frequencies are reduced. Thus, a more important lifetime of the batteries can be expected.

Fig. 9(b) shows the reference mission of the flywheel ($P_{\mathrm{FWref}} = P_{\mathrm{FWref0}} + P_{\mathrm{FWS}}$) and its response. The state of charge and the flywheel mission in Ragone's plan are also shown in this figure. The flywheel response follows its reference mission, except for some acceptable saturation in terms of charge power. The representation of the flywheel response in Ragone's plan shows that the storage device is optimized, because it is close to the saturation limit of discharge, which is related to the choice of management frequency. However, in charge, the flywheel presents much saturation. The state of charge varies from 30% to 100%. Compared with the first management strategy where the flywheel is not well used in terms of energy, the second management strategy allows better exploitation of the flywheel, on the one hand, by injecting parts of low-frequency missions and, on the other hand, by amplifying high-frequency mission by the decrease in the cutoff frequency ($F_g = 17$ mHz). Indeed, the minimal state of charge goes from 77% to 30%. This clearly appears in Ragone's plan, where the flywheel response, for the same daily mission, spreads out even more in the useful zone of the flywheel defined by its operating limits.

Fig. 14 shows that the batteries are able to supply all the required power. They undergo saturations in the case of maximal power of charge ($P_{\mathrm{BT\,ch\,max}} = -97.2$ kW) or when the batteries are totally charged. The diesel generator perfectly follows its reference mission. The dynamics of this last one are supposed to be rather fast with regard to the variations of its reference mission. The diesel generator works according to three different modes: with its maximum charge (236 kW), with batteries of maximum charge power (97.2 kW), and for the stop mode when the batteries are totally charged and the locomotive is stopped.

VII. Systemic Comparison of Flywheel- and Ultracapacitor-Based Architectures

A. Geometric Sizing Model

The global volume available for the embedded energetic sources and their associated devices (static converters, thermal radiators, and filter elements) is about 32 m^3. Therefore, the

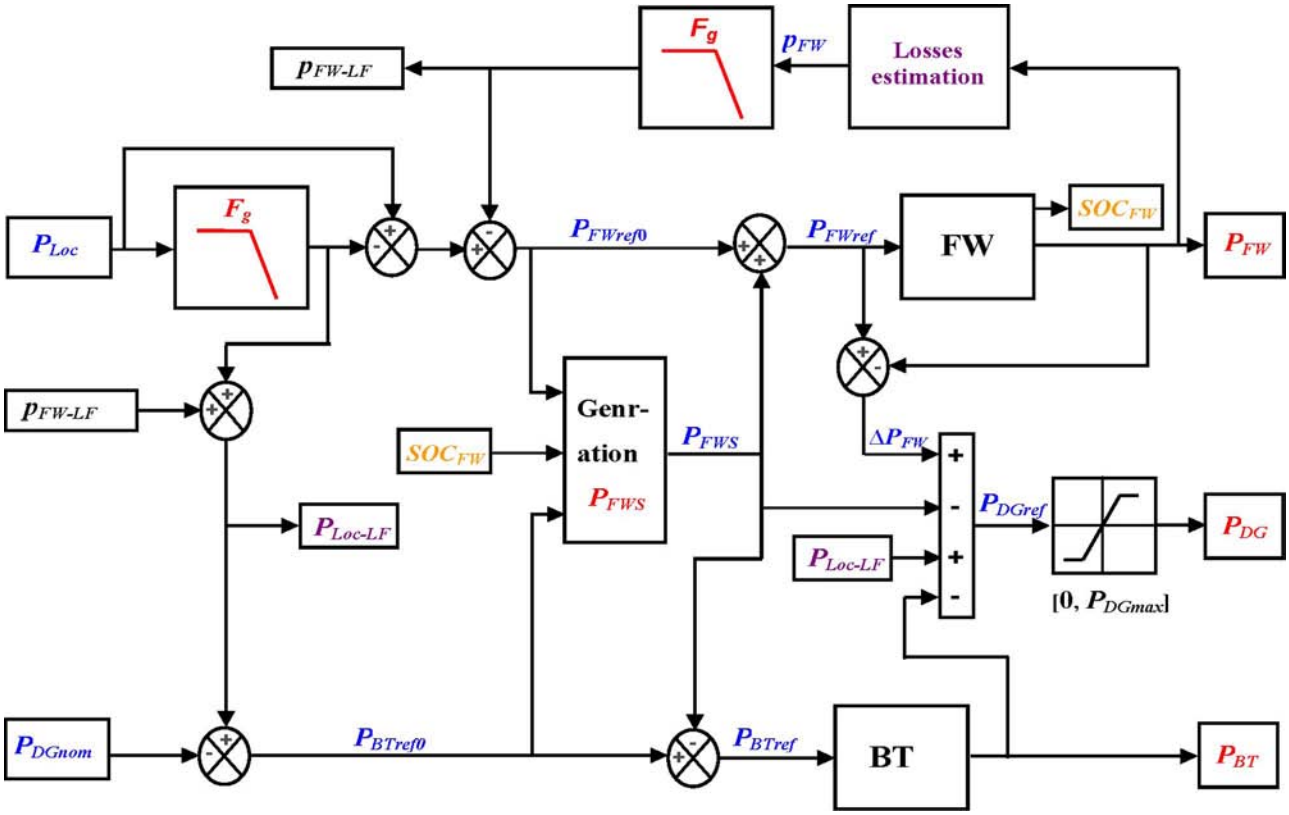

Fig. 13. Synoptic scheme of the optimized energy-management strategy.

volume of each component has been estimated with relations obtained from manufacturer data to fulfill space constraints. The diesel generator volume Ω_{DG} (in cubic meters) has been interpolated with a linear function as follows:

$$\Omega_{\mathrm{DG}} = 3 \times 10^{-5} P_{\mathrm{DGN}} + 0.03. \tag{4}$$

The ultracapacitor and battery volumes (i.e., Ω_{BT} and Ω_{SC}, respectively) are calculated from the corresponding unit cell volumes (i.e., Ω_{BT0} and Ω_{SC0}, respectively), considering the total number of cells and by means of assembly coefficients λ_{BT} and λ_{SC}, i.e.,

$$\begin{cases} \Omega_{\mathrm{BT}} = \lambda_{\mathrm{BT}} \times \mathrm{NP_{BT}} \times \mathrm{NS_{BT}} \times \Omega_{\mathrm{BT0}} \\ \Omega_{\mathrm{SC}} = \lambda_{\mathrm{SC}} \times \mathrm{NP_{SC}} \times \mathrm{NS_{SC}} \times \Omega_{\mathrm{SC0}} \end{cases} \tag{5}$$

where $\Omega_{\mathrm{BT0}} = 4.33 \times 10^{-3}$ m^3; $\Omega_{\mathrm{SC0}} = 9.9 \times 10^{-4}$ m^3; $\mathrm{NP_{BT}}$ and $\mathrm{NS_{BT}}$ are the number of parallel and series battery cells, respectively; and $\mathrm{NP_{SC}}$ and $\mathrm{NS_{SC}}$ are the number of parallel and series ultracapacitor cells, respectively.

The assembly coefficients, which take into account of the interspaces between each cell, the volume of the static converters, and the corresponding cooling devices, are estimated to be $\lambda_{\mathrm{BT}} = 1.9$ and $\lambda_{\mathrm{SC}} = 2.58$ [1].

The flywheel volume, including that of motor/generator, static converter, and safety envelope, is given by the manufacturer

$$\Omega_{\mathrm{FW}} = 2.3 \times 1.4 \times 0.514 = 1.655 \text{ m}^3. \tag{6}$$

Global system volume Ω_{Σ} is then

$$\begin{cases} \Omega_{\Sigma} = \Omega_{\mathrm{DG}} + \Omega_{\mathrm{BT}} + \Omega_{\mathrm{SC}}, & \text{with SC architecture} \\ \Omega_{\Sigma} = \Omega_{\mathrm{DG}} + \Omega_{\mathrm{BT}} + \Omega_{\mathrm{FW}}, & \text{with FW architecture.} \end{cases} \tag{7}$$

B. Battery and Ultracapacitor Lifetime Models

The battery lifetime model is related to the number of cycles to failure c_F, which can be expressed as a function of the depth of discharge (DOD, which is specified in percent) [25]. A qualitative approximation of the c_F coefficient has been derived in [1] for the Hoppecke FNC 1502HR battery cells for rated conditions (i.e., the temperature between 30 °C and 40 °C, charge at C_5, and discharge at $2C_5$) as follows:

$$c_F(\mathrm{DOD}) = 966 \times \mathrm{DOD}^{-2.37}. \tag{8}$$

Considering the number of cycles to failure for DOD $= 100\%$ as a reference, we can express a "cycle weight" w_{CYCLE} for lower DODs as

$$w_{\mathrm{CYCLE}}(\mathrm{DOD}) = \frac{c_F(100\%)}{c_F(\mathrm{DOD})}. \tag{9}$$

This weight evaluates the effect of a cycle for a given DOD in relation to a cycle for full DOD. Since battery SOC characteristics during a particular driving mission generally consist of various cycles with different DODs, a global battery stress estimator $\mathrm{LFT_{BT}}$ evaluates the battery lifetime from the total number of cycles N_{CYCLE} at a given DOD. To compute this estimator, the DOD range is divided into ten uniformly spaced intervals. Then, the number of cycles $N_{\mathrm{CYCLE}}(i)$, which occurs in a DOD interval i, is determined from the battery SOC associated with the locomotive mission. Finally, the $\mathrm{LFT_{BT}}$ estimator is calculated by globalizing all cycles in all intervals,

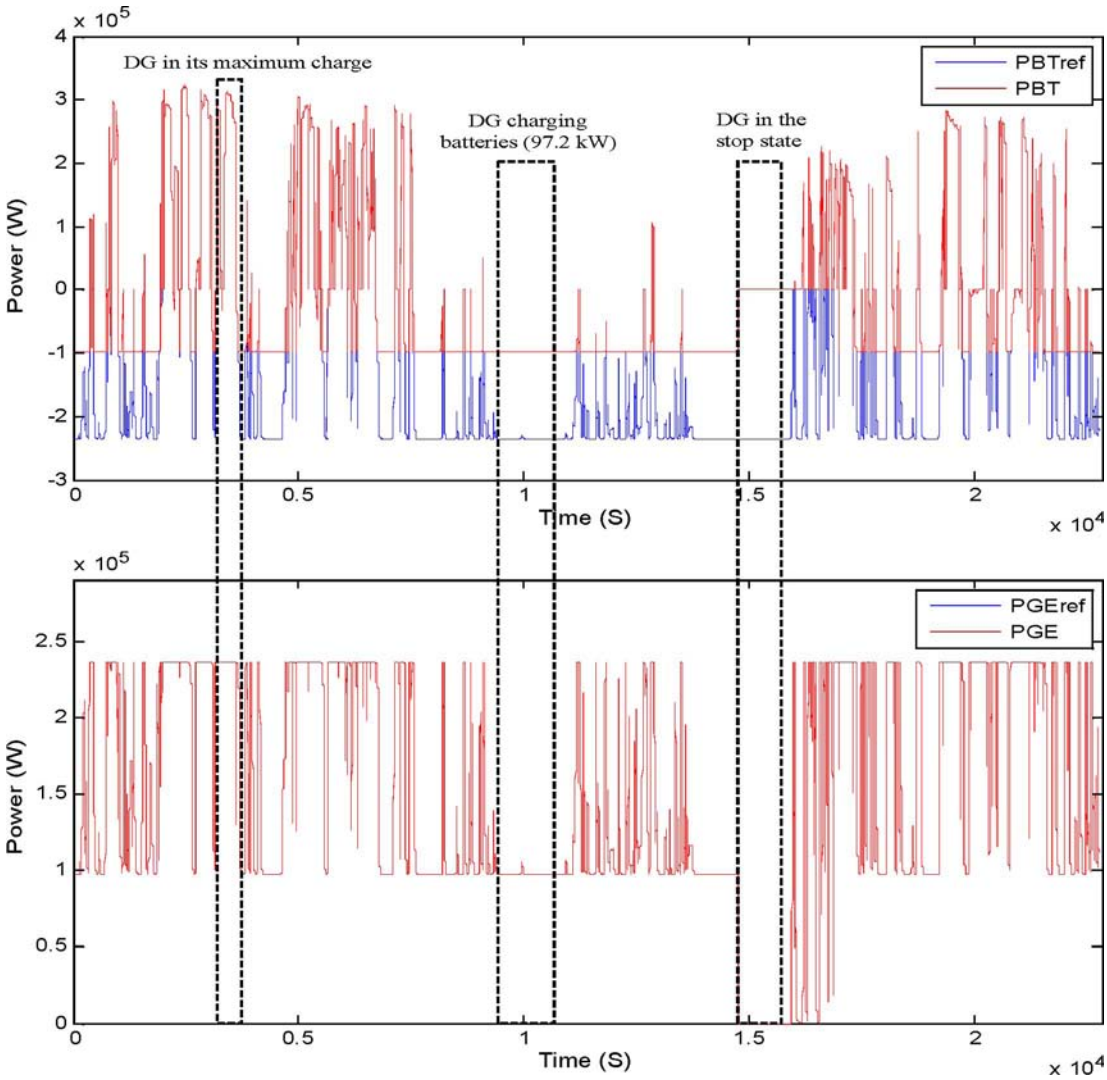

Fig. 14. Reference mission and corresponding response of the batteries and diesel generator.

taking account of their weight according to the corresponding DOD, i.e.,

$$\mathrm{LFT_{BT}} = \sum_{i=1}^{10} w_{\mathrm{CYCLE}}(i) \times N_{\mathrm{CYCLE}}(i) \qquad (10)$$

where $w_{\mathrm{CYCLE}}(i)$ denotes the cycle weight at the middle of the considered DOD interval i. The same approach is used to calculate the ultracapacitors' lifetime, considering linear distributed weights and a cycle to failure reference of 500 000 at 100% of DOD.

The computation of the cycle number is based on the "Rainflow counting method." More details about this method can be found in [1] and [26]. Note that the $\mathrm{LFT_{BT}}$ estimator is a criterion that neglects microcycles. The latter are the cycles with a depth lower than 1% of the maximal storage capacity.

C. Comparison

The above comparison is based on the locomotive power mission of Fig. 7. It shows that the existing solution S_{ex} for the hybrid locomotive and the two flywheel based solutions with basic and optimized management strategy (S_{FW1} and S_{FW2}, respectively) present rather close consumptions (see Table III and Fig. 15). This last solution (S_{FW2}) guarantees PLATHEE Project objectives in terms of quantity of emitted CO_2. The number of battery cycles is the same for both solutions S_{ex} and S_{FW2} while neglecting the microcycles and is a little higher for S_{FW1}, because the cutoff frequency is larger. However, we can declare that the number of microcycles (the cycles with a depth lower than 1% of the maximal storage capacity) supported by the batteries with the S_{FW2} solution is more important than that obtained with the existing solution S_{ex}. Note that the number of microcycles on the battery cells is increased when the cutoff frequency is enlarged. According to the technology and the type of batteries, microcycles can degrade the battery lifetime. Note also that 7 kWh energy storage by means of ultracapacitors has been replaced by 4 kWh energy storage with a flywheel, which can explain the difference between both solutions in terms of the filtering frequency and consequent microcycles.

Flywheel solution S_{FW2} is advantageous from the point of view of the lifetime [14], [15] and the system volume. It allows reducing the volume by 2.4 $\mathrm{m^3}$, compared with the locomotive existing solution, and 0.9 $\mathrm{m^3}$, compared with the

TABLE III
FEASIBILITY CONSTRAINTS AND THE PERFORMANCE CRITERIA

	S_{ex}: existing solution with SC (F_g=5 mHz)	S_{FW1}: Basic strategy with FW (F_g=27mHz)	S_{FW2}: optimized strategy with FW (F_g=17mHz)
Cut-off frequency F_g	5 mHz	27 mHz	17 mHz
Nb of battery cells	1200	1312	1200
Nb of SC cells	1600	–	–
System volume (m^3)	16.5	14.9	14
Fuel Burn (L)	198	203	201

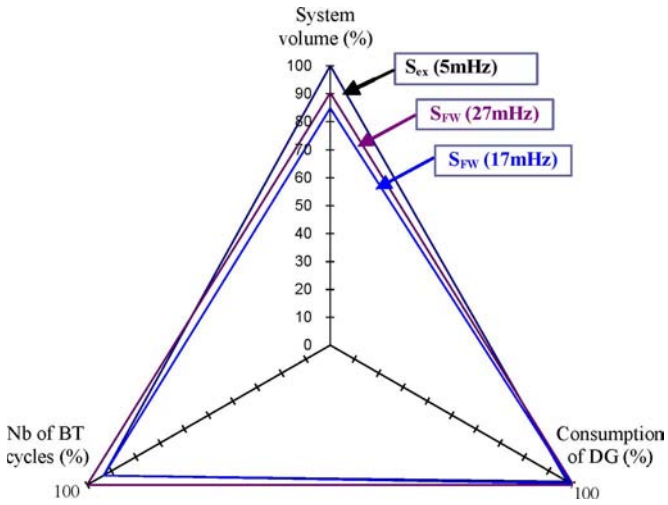

Fig. 15. Comparison according to the feasibility constraints and the performance criteria.

flywheel-based solution with basic management strategy S_{FW1}. In addition, the number of chemical elements to be recycled is much more important with the existing solution (1200 BT + 1600 SC with the existing solution/1200 BT with flywheel solution).

VIII. CONCLUSION

In this paper, a power flow model of the whole traction device (diesel generator and energy storage elements) has been proposed as an efficient design tool for a "system approach." The principle of the energy-management strategy based on a frequency approach has also been described. In a second part, the integration of a flywheel device as element of energy storage on the hybrid locomotive in complement with the diesel generator and the batteries is studied. This study is made according to two energy-management strategies based on the frequency approach. The first strategy is identical to that previously used in the existing design solution with ultracapacitors: The flywheel only supplies high-frequency harmonics. This has resulted in a nonoptimal exploitation of the flywheel and an increase in the battery cell number. With the aim of optimizing the use of flywheel and, afterward, the sizing of the locomotive, a second energy management strategy has been proposed. It consists of injecting a part of the low-frequency mission of the batteries into the flywheel while keeping priority for its high-frequency mission. This last strategy allows decreasing the cutoff frequency and, thus, decreasing the number of battery cells and improving their lifetime. At the end, a comparative study of the present hybrid solution and the proposed solution according to a set of feasibility constraints and performance criteria has been presented. Consequently, the proposed solution S_{FW2} (215 kW diesel engine, 5.33 kWh/325 kW flywheel, and 1200 cells of batteries) with the optimized management strategy is a good candidate for the realization of a future hybrid locomotive.

Even though the locomotive sizing is based on local optimization methodology, the overall system optimization is not guaranteed. Thus, the hybrid locomotive sizing can be investigated using a multiobjective optimization strategy. The criteria to be optimized could be the global system cost of the energetic sources and the carbon dioxide quantity emitted by a diesel locomotive. Eventually, hybrid systems can be extended to new railway segments, such as "last mile locomotive," auxiliaries of high-speed trains, hybrid tramways, and metros.

REFERENCES

[1] C. R. Akli, "Conception systémique d'une locomotive hybride autonome," Ph.D. dissertation, INP Toulouse, Toulouse, France, Jun. 2008.

[2] F. W. Donnelly, R. L. Cousineau, and R. N. M. Horsley, "Hybrid technology for the rail industry," in *Proc. ASME/IEEE Joint Rail Conf.*, Baltimore, MD, Apr. 6–8, 2004, pp. 113–117.

[3] R. L. Cousineau, "Development of a hybrid switcher locomotive the railpower green goat," *IEEE Instrum. Meas. Mag.*, vol. 9, no. 1, pp. 25–29, Feb. 2006.

[4] C. R. Akli, X. Roboam, B. Sareni, and A. Jeunesse, "Energy management and sizing of a hybrid locomotive," in *Proc. 12th EPE*, 2007, pp. 8–49.

[5] W. Koczara, L. Grzesiak, and M. da Ponte, "Novel hybrid load-adaptive variable speed generating set," in *Proc. IEEE ISIE*, 1998, pp. 271–273.

[6] W. Koczara, L. Grzesiak, and M. da Ponte, "Hybrid load-adaptive variable-speed generating set: New system topology and control strategy," in *Proc. Int. Conf. Power Gener.*, Dec. 1998, pp. 6–54.

[7] W. Koczara, L. Grzesiak, and M. da Ponte, "Hybrid generator apparatus," South African Patent Application 97/11503, Dec. 22, 1997.

[8] L. Grzesiak, W. Koczara, P. Pospiech, and M. da Ponte, "Power quality of the hygen autonomous load-adaptive adjustable-speed generating system," in *Proc. APEC*, 1999, pp. 945–946.

[9] M. Osawa, *The Ne@Train, First Hybrid Material in the World*. Bruxelles, Belgium: Rail International, 2004, pp. 9–86.

[10] D. Briginshaw, "Hybrid traction system benefits environment: Japan's new energy train project uses a hybrid diesel-electric traction system to achieve major reductions in energy consumption, noxious emissions, and noise," *Int. Railway J.*, Dec. 1, 2004.

[11] [Online]. Available: http://www.citadismag.transport.alstom.com, Feb. 2008.

[12] M. Thiounn, "PLATHEE—A platform for energy efficiency and environmentally friendly hybrid trains," in *Proc. 8th World Congr. Railway Res.*, Seoul, Korea, May 18–22, 2008. Paper R.3.4.3.3.

[13] P. E. Kascak, B. H. Kenny, T. P. Dever, and W. Santiago, "International space station bus regulation with NASA Glenn research center flywheel energy storage system development unit," in *Proc. Intersoc. Energy Convers. Conf.*, Savannah, GA, Jul. 29–Aug. 2, 2001, pp. 1–2. NASA/TM-2001-211138.

[14] R. Hebner, J. Beno, and A. Walls, "Flywheel batteries come around again," *IEEE Spectr.*, vol. 39, no. 4, pp. 46–47, Apr. 2002.

[15] A. J. Rudell, *Flywheel Energy Storage Renewable Energy Systems*. Chilton, U.K.: CCLRC Rutherford Appleton Lab.

[16] N. Bernard, H. Ben Ahmed, B. Multon, C. Kerzreho, J. Delamare, and F. Faure, "Flywheel energy storage systems in hybrid and distributed electricity generation," in *Proc. Power Quality*, Nuremberg, Germany, May 2003, pp. 121–130.

[17] R. L. Hockney and C. A. Driscoll, *Powering of Standby Power Supplies Using Flywheel Energy Storage*. Cambridge, MA: Beacon Power, pp. 105–107.

[18] [Online]. Available: http://www.fptpowertrain.com/eng/home.htm, Jun. 2007.
[19] L. A. Graham, "Greenhouse gas emissions from light duty vehicles under a variety of driving conditions," in *Proc. IEEE EIC Climate Change Technol.*, 2006, pp. 1–8.
[20] [Online]. Available: http://www.hoppecke.com/, Mar. 2008.
[21] D. Bonta, V. Tulbure, and C. Festila, "Diesel-engine intelligent control in railway traction," in *Proc. IEEE Int. Conf. Autom., Quality, Test., Robot.*, May 2006, vol. 1, pp. 318–320.
[22] P. Mestre and S. Astier, "Utilization of ultracapacitors as an auxiliary power source in electrical vehicle," in *Proc. EPE*, 1997, pp. 4.670–4.673.
[23] T. Christen and C. Olher, "Optimizing energy storage devices using Ragone plots," *J. Power Sources*, vol. 110, no. 1, pp. 107–116, Apr. 2002.
[24] C. R. Akli, X. Roboam, B. Sareni, and A. Jeunesse, "Integrated optimal design of a hybrid locomotive with multiobjective genetic algorithms," in *Proc. 10th Int. Workshop OIPE*, Ilmenau, Germany, Sep. 15–17, 2008. Selected for publication in the *Int. J. Applied Electromagn. Mech.*, 2009.
[25] S. Drouilhet and B. L. Johnson, "A battery life prediction method for the hybrid power applications," presented at the 35th AIAA Aerospace Sciences Meeting Exhibit, Reno, NV, 1997, Paper AIAA-1997-948.
[26] S. H. Baek, S. S. Cho, and W. S. Joo, "Fatigue life prediction based on the rainflow cycle counting method for the end beam of a freight car bogie," *Int. J. Autom. Technol.*, vol. 9, no. 1, pp. 95–101, Feb. 2008.

Amine Jaafar was born in Sousse, Tunisia, in 1983. He received the Engineering degree in electrical engineering from the Ecole Nationale d'Ingénieur de Monastir, Monastir, Tunisia, in 2007 and the Master Research degree from the Institut National Polytechnique de Toulouse, Université de Toulouse, Toulouse, France, in 2008. He is currently working toward the Ph.D. degree with the Institut National Polytechnique of Toulouse.

Cossi Rockys Akli received the Ph.D. degree in electrical engineering from the Institut National Polytechnique de Toulouse, Université de Toulouse, Toulouse, France, in 2008. His doctoral dissertation was supported by the PLATHEE Project with the aim of defining the global architecture, the element sizing, and the energy-management strategy of the hybrid locomotive.

He is currently an Electrical Engineer with ALSTOM Transport Tarbes, Semeac, France.

Bruno Sareni was born in Bron, France, in 1972. He received the Ph.D. degree from the Ecole Centrale de Lyon, Ecully, France, in 1999.

He is currently with the Institut National Polytechnique de Toulouse, Université de Toulouse, Toulouse, France, where he is an Assistant Professor with the Electrical Engineering and Control Systems and a Researcher with the Laboratory on Plasma and Conversion of Energy. His research interests include the analysis of complex heterogeneous power devices in electrical engineering and the optimization of these systems using artificial evolution algorithms.

Xavier Roboam received the Ph.D. degree in electrical engineering from the Institut National Polytechnique de Toulouse, Université de Toulouse, Toulouse, France, in 1991.

Since 1992, he has been with the Laboratory on Plasma and Conversion of Energy, Institut National Polytechnique de Toulouse, as a Full-Time Researcher. Since 1998, he has been the Head of the Research Group in Electrical Energy and Systemics, whose objective is to process the design problem in electrical engineering at a "system level." He develops methodologies that are specifically oriented toward multifield systems design for applications, such as electrical embedded systems or renewable-energy systems.

Alain Jeunesse received the Engineering degree in electrical engineering from the Ecole Supérieure d'Ingénieurs en Electronique et Electrotechnique, Paris, France, in 1976.

Since 1977, he has been with the Centre d'Ingénierie du Materiel du Mans, Le Mans, France, where he was an electrical engineer with the French National Railways Company and the Head of the Railway Traction and Electromagnetic Compatibility Unit, where he is currently a Scientific Advisor on railway traction systems.